

Orthonormal Divergence-free Wavelet Analysis of Energy Transfer in Magnetohydrodynamic Turbulence

Keisuke ARAKI and Hideaki MIURA¹⁾

Okayama University of Science, 1-1 Ridai-cho, Okayama, OKAYAMA 700-0005 JAPAN

¹⁾*National Institute for Fusion Science, Oroshi-cho Toki, GIFU 509-5292 JAPAN*

(Received: 1 September 2008 / Accepted: 11 January 2009)

For the purpose of clarifying mechanism of local structure formations in magnetohydrodynamic (MHD) turbulence, energy transfers among various scales and positions of magnetic/kinetic energies in the course of roll-up processes of vortices are studied by direct numerical simulations (DNS) and orthonormal wavelet analysis. Initial shear layers are perturbed by three-dimensional random perturbations, and roll up to form tubular vortices which are connected to each other by blade structures. The energy transfers in this process is considered to be modified from that in the neutral fluid turbulence in the presence of large-scale magnetic fields. Information on scales provided by the wavelet analysis are used to study scale-to-scale energy transfers in the roll-up processes. The scale-to-scale analysis suggests that large scale flow structures directly excite magnetic fields with various scales. Energy exchange between the kinetic and magnetic field energies will also be examined from the points of views of local analysis of scale-to-scale energy transfers.

Keywords: Wavelet analysis, turbulence, coherent structures, scale-to-scale energy transfer, nonlocal interaction

1. Introduction

Turbulent motions of plasmas are considered to play key roles in magnetic confinement system. For example, the plasma and energy transports across the magnetic field lines are closely related to turbulence[1]. For a neutral fluid, turbulent transport of kinetic energy is well known as “turbulent energy cascade” and its dynamical mechanism has been intensively investigated (cf.Refs.[2, 3]). In terms of wavelet analysis, Kishida et al. have found that local interaction dominates the transfer process[5]. For MHD fluids, Alexakis et al. have carefully conducted DNS studies and investigated turbulent energy transfer processes between the velocity and magnetic fields and between larger and smaller scales [6] and similar analysis is carried out for Hall-MHD case[7]. They found that nonlocal interaction is important for the energy supplying process from the kinetic energy to the magnetic one.

In the present study, we will focus the relation between motions of some isolated coherent structures and magnetic induction process under the existence of a uniform background magnetic field, which is not treated in Refs.[6, 7]. For this purpose, wavelet analysis, which captures the information of spatial scale and position simultaneously, is adopted. We use here orthonormal divergence-free wavelet, which demonstrates clearly that coherent structures are relevant to the energy transfer process[8]. In the present study we use only the scale information of wavelets and analyze scale-to-scale energy transfer.

2. Basic equations

Incompressible MHD equations are described as

$$\frac{\partial \mathbf{u}}{\partial t} = -(\mathbf{u} \cdot \nabla) \mathbf{u} - \nabla p + \mathbf{j} \times \mathbf{B} + \nu \nabla^2 \mathbf{u}, \quad (1)$$

author's e-mail: araki@are.ous.ac.jp

$$\frac{\partial \mathbf{B}}{\partial t} = \nabla \times [\mathbf{u} \times \mathbf{B}] + \eta \nabla^2 \mathbf{B} \quad (2)$$

$$\nabla \cdot \mathbf{u} = 0 \quad (3)$$

where \mathbf{B} is the magnetic field (normalized by a representative value B_0), $\mathbf{j} = \nabla \times \mathbf{B}$ is the current (normalized by B_0/L_0 ; L_0 is the characteristic length), \mathbf{u} is the velocity (normalized by the Alfvén speed $V_A = B_0/\sqrt{\mu_0 n_i M_i}$; μ_0 is the permeability of vacuum, M_i is the ion mass and n_i is the ion number density, which is assumed to be constant for simplicity), ν is the viscosity and η is the resistivity (normalized by $V_A L_0$), and p is the pressure (normalized by B_0^2/μ_0). The pressure p is given as the solution of the Poisson equation which comes from the divergence of eq.(1).

3. Numerical method

A DNS is carried out using pseudospectral method with 512^3 number of grids in physical space, whose system length is 2π in each direction, and 2/3-dealiasing method for the mode interaction calculation and using Runge-Kutta-Gill method for time stepping [4]. The kinematic viscosity and normalized resistivity are set to $\nu = \eta = 0.001$. The initial condition is a uniform magnetic field given by $\mathbf{B}_0 = (0, 0, 0.1)$ and a pair of shear layers given by

$$\mathbf{u} = \left(0.33 \left(\arctan\left(\frac{32}{\pi}\left(y - \frac{\pi}{4}\right)\right) - \arctan\left(\frac{32}{\pi}\left(y - \frac{3\pi}{4}\right)\right) - 1.54 \right), 0, 0 \right)$$

with small isotropic disturbances whose Fourier spectrum is given by $E(k) \propto \left(\frac{k}{k_0}\right)^2 \exp\left[-\left(\frac{k}{k_0}\right)^2\right]$. No forcing is introduced during the calculation.

While the DNS is carried out in terms of Fourier

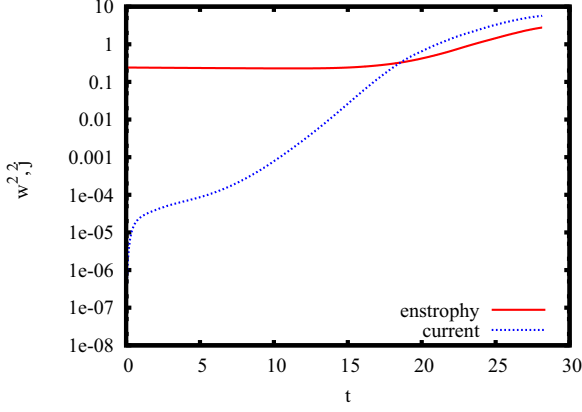


Fig. 1 Time development of enstrophy and current. In the present work the amplitudes of quantities are measured in dimensionless units that are normalized by the constants given in §2.

modes, the mode interaction analysis is carried out in terms of wavelet modes. Orthonormal divergence-free wavelets, which we call “helical wavelets” and denote by $\tilde{\psi}_{j\epsilon\vec{l}\sigma}(\vec{x}, t)$ hereafter, are obtained by a unitary transform of complex helical waves[5]. The velocity and magnetic fields are expanded in helical wavelet modes as follows:

$$\mathbf{f}(\vec{x}, t) = \sum_{j,\epsilon,\vec{l},\sigma} \tilde{\mathbf{f}}_{j\epsilon\vec{l}\sigma}(\vec{x}, t). \quad (4)$$

where \mathbf{f} stands for \mathbf{u} or \mathbf{B} , $\tilde{\mathbf{f}}_{j\epsilon\vec{l}\sigma}(\vec{x}, t)$ is a helical wavelet mode which is given by

$$\tilde{\mathbf{f}}_{j\epsilon\vec{l}\sigma}(\vec{x}, t) := \tilde{\mathbf{f}}_{j\epsilon\vec{l}\sigma}(t) \tilde{\psi}_{j\epsilon\vec{l}\sigma}(\vec{x}), \quad (5)$$

$$\tilde{\mathbf{f}}_{j\epsilon\vec{l}\sigma}(t) := \int \mathbf{f}(\vec{x}, t) \cdot \tilde{\psi}_{j\epsilon\vec{l}\sigma}(\vec{x}) d^3\vec{x}, \quad (6)$$

and $j, \epsilon, \vec{l}, \sigma$ are the indices of helical wavelet. The implication of indices are summarized in Ref.[8].

4. Numerical result

Time development of the enstrophy and current are shown in Fig.1. Disturbances are grown gradually and formation of rolling-up vortices become prominent around $t = 15$. About $t = 18$ and the later time the net current exceeds the enstrophy. We analyzed mode interactions at the time $t = 16, 18, 20, 22$ and show the result of $t = 22$ in the following.

Fourier and wavelet scale spectra of the velocity and magnetic fields at $t = 22$ is shown in Fig.2 and the enstrophy and current density fields are shown in Fig.3. In Fig.2 Fourier kinetic and magnetic energy spectra are drawn simultaneously with wavelet ones in order to compare the amplitude of wavelet spectra and spatial scale of wavelets with Fourier ones which may be more familiar to the readers.

At this time, the lowest wavenumber Fourier modes, i.e. large scale flow structures have most of energy and for

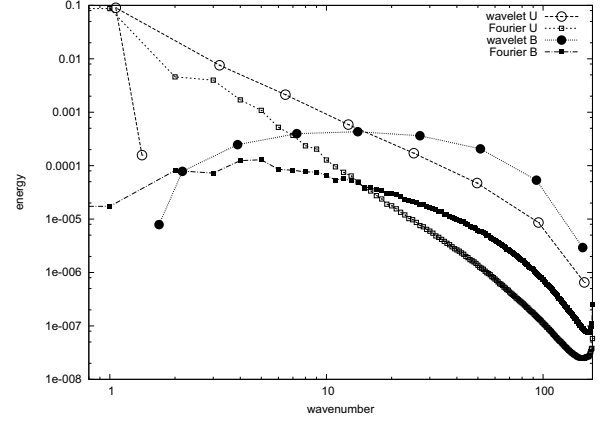


Fig. 2 Fourier and wavelet scale spectra of kinetic and magnetic energy. Open and solid symbols denote the kinetic and magnetic energy spectra, respectively. The abscissa of each wavelet spectrum is determined by the mean wavenumber $k := \sqrt{\int |\nabla \times \mathbf{f}|^2 d^3\vec{x} / \int |\mathbf{f}|^2 d^3\vec{x}}$ where \mathbf{f} stands for \mathbf{u}_j or \mathbf{B}_j .

larger wavenumbers the magnetic energy become larger than the kinetic one. Several strong vortices are developed around the initial shear layers and current is developed around the vortices and the shear layers between them. It is expected that the fields have some characteristic features of interactions between the velocity and magnetic fields driven by coherent structures.

4.1 Energy budget in wavelet scale spectra representation

Taking inner product of Eqs.(1) and (2) with helical wavelet modes and summation with respect to all the indices but j , which implies spatial scale in physical space, we obtain energy budget equations with respect to the wavelet scale spectra

$$\frac{d}{dt} E_j^{(u)} = N_j + L_j + L_j^{(0)} + D_j, \quad (7)$$

$$\frac{d}{dt} E_j^{(B)} = I_j + I_j^{(0)} + R_j \quad (8)$$

where the terms $N_j, L_j, L_j^{(0)}, D_j, I_j, I_j^{(0)}$, and R_j are the inner product with $-(\mathbf{u} \cdot \nabla)\mathbf{u}$, $(\nabla \times \mathbf{B}) \times \mathbf{B}$, $(\mathbf{B}_0 \cdot \nabla)\mathbf{B}$, $\nu \nabla^2 \mathbf{u}$, $\nabla \times (\mathbf{u} \times \mathbf{B})$, $(\mathbf{B}_0 \cdot \nabla)\mathbf{u}$, and $\eta \nabla^2 \mathbf{B}$, respectively. The pressure term is vanished because helical wavelet modes are divergence-free.

The contribution of each term to the energy budget of kinetic and magnetic fields is shown in Fig.4. Velocity field loses its energy at the scale with wavelet scale index $j = 1$, at which the kinetic energy spectrum has its peak, and the other scales it acquires energy. On the other hand, magnetic field acquires energy at all the scales. That is, the fields are in such a process that the energy is redistributed from the $j = 1$ mode of the velocity field to the other wavelet modes of the velocity and magnetic fields as a whole.

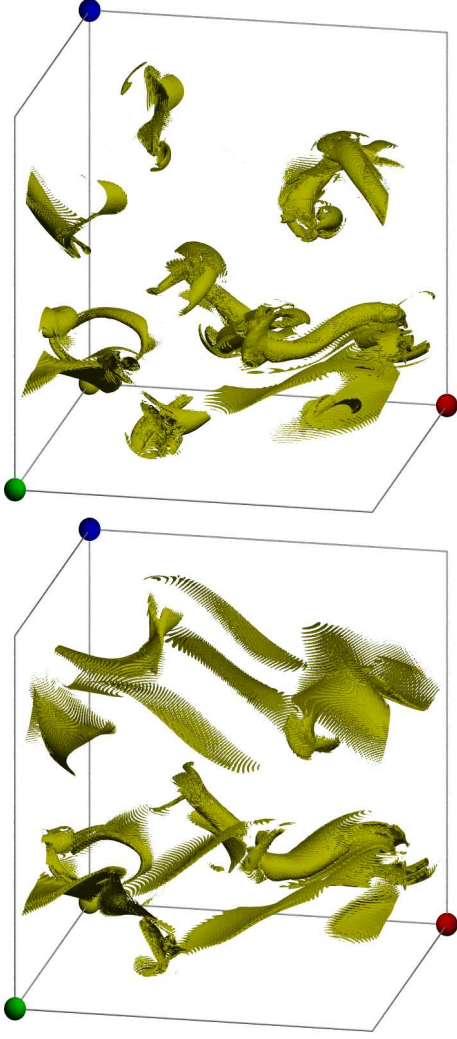


Fig. 3 Isosurfaces of enstrophy density (top) and current density (bottom)

The fluid motion is most affected by the nonlinear interaction for larger scales ($j \leq 5$) and Alfvén wave for smaller scales ($j \geq 6$). As for the contribution of Lorentz force term to the kinetic energy budget L_j , Lorentz force reduces the kinetic energy at $0 \leq j \leq 4$ and $j = 7$. This implies that the motion of fluid induces magnetic field as a whole though some small backscatter from magnetic to kinetic energy is seen at $j = 5, 6$ and 8 .

The energy budget due to the Alfvén waves $L_j^{(0)}$ and $I_j^{(0)}$ tend to transport the energy from velocity field to magnetic one for larger spatial scales cases ($j \leq 2$). For smaller scales ($j \geq 3$) the tendency become opposite. This implies that Alfvén wave suppresses the growth of smaller scales of the magnetic field. This feature is also seen at the earlier times $t = 16, 18, 20$.

4.2 Inter-scale mode interaction between u_j and b_j

Next we will see the debit and credit relation between the kinetic and magnetic scale energy spectra $E_j^{(u)}$ and $E_k^{(B)}$.

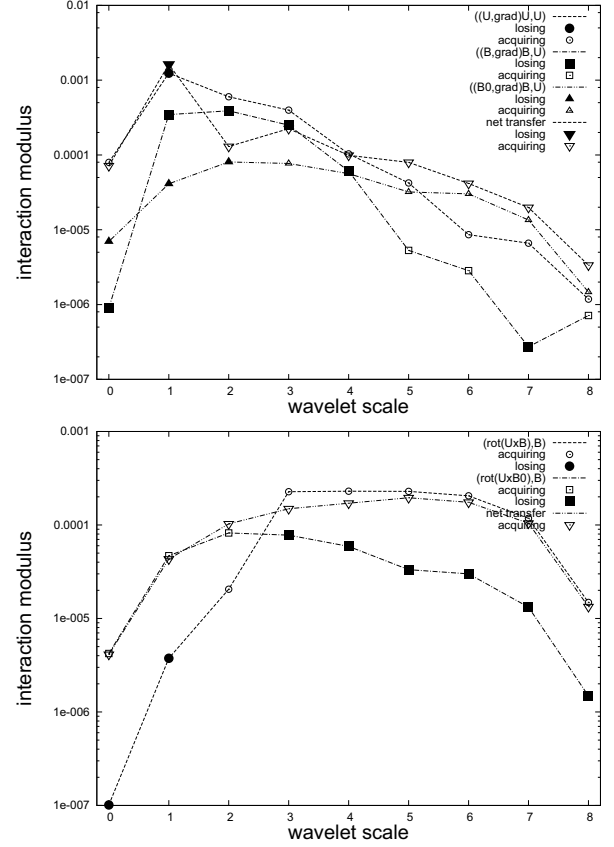


Fig. 4 Wavelet spectra of kinetic and magnetic energy budget equations at the time $t = 22$; (top) the kinetic energy budget, (bottom) magnetic one. Ordinate of each plot is determined by the modulus of each term and the sign of it is shown by open (acquiring) or solid (losing) symbols.

For this purpose the mode interaction terms that appear in the rhs of the energy budget equations (7) and (8) are decomposed into subcomponents as follows: $N_j = \sum_k N_{jk}$, $L_j = \sum_k L_{jk}$, $L_j^{(0)} = \sum_k L_{jk}^{(0)}$, $I_j = \sum_k I_{jk}$, $I_j^{(0)} = \sum_k I_{jk}^{(0)}$ where the subcomponents are defined by

$$N_{jk} = - \int \mathbf{u}_j \cdot (\mathbf{u} \cdot \nabla) \mathbf{u}_k d^3 \vec{x}, \quad (9)$$

$$L_{jk} = \int \mathbf{u}_j \cdot (\nabla \times \mathbf{B}_k) \times \mathbf{B} d^3 \vec{x}, \quad (10)$$

$$L_{jk}^{(0)} = \int \mathbf{u}_j \cdot (\mathbf{B}_0 \cdot \nabla) \mathbf{B}_k d^3 \vec{x}, \quad (11)$$

$$I_{jk} = \int \mathbf{B}_j \cdot \nabla \times (\mathbf{u}_k \times \mathbf{B}) d^3 \vec{x}, \quad (12)$$

$$I_{jk}^{(0)} = \int \mathbf{B}_j \cdot (\mathbf{B}_0 \cdot \nabla) \mathbf{u}_k d^3 \vec{x}. \quad (13)$$

These subcomponents are carefully defined to satisfy the balance conditions

$$N_{jk} = -N_{kj}, \quad (14)$$

$$L_{jk} = -I_{kj}, \quad (15)$$

$$L_{jk}^{(0)} = -I_{kj}^{(0)}. \quad (16)$$

The first balance equation (14) implies the energy debit and credit between the budget of the kinetic energies $E_j^{(u)}$ and

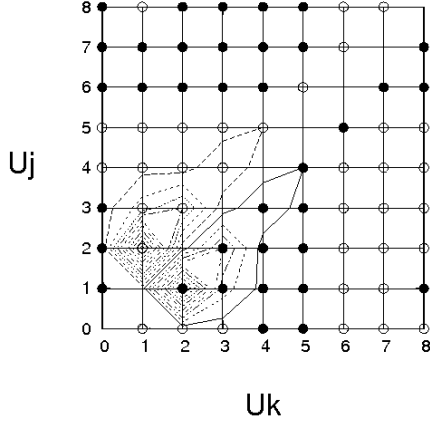


Fig. 5 Wavelet spectra of nonlinear kinetic energy transfer N_{jk} . Solid circles: $N_{jk} < 0$, i.e. energy is transferred from \mathbf{u}_j to \mathbf{u}_k ; open circles: $N_{jk} > 0$. Contours are drawn at $-0.95, -0.85, \dots, 0.85, 0.95$ of $\max\{|N_{jk}|\}$ to grasp the amplitude of N_{jk} visually.

$E_k^{(u)}$ is exactly balanced by the modulus of N_{jk} . The rest two equations (15) and (16), on the other hand, imply the energy balance relation between the budget of the kinetic and magnetic energies $E_j^{(u)}$ and $E_k^{(B)}$.

Distribution of scale-to-scale wavelet nonlinear energy transfer N_{jk} is shown in Fig.5. Since N_{jk} satisfies the balance condition (14), the graph is odd with respect to the line $j = k$. If N_{jk} has positive value at (j, k) , it implies that energy is transferred from $E_j^{(u)}$ to $E_k^{(u)}$ by N_{jk} . Since positive peaks are aligned at $k = j + 1$, the following two characteristics are concluded: (1) energy is transferred from larger scales to smaller ones, and (2) the dominant nonlinear transfers are local. Although the flow is not fully developed turbulent state but has only several large rolling-up vortices, this tendency is quite similar to that of fully developed three dimensional turbulent flow [5].

Energy transfer between the velocity and magnetic fields by magnetic induction L_{jk} is shown in Fig.6. It is remarkable that, irrespective of the scale of magnetic field, transfer to the magnetic energy is induced by the large scale wavelet modes of the velocity field, i.e. $\mathbf{u}_1, \mathbf{u}_2$ and \mathbf{u}_3 . This result directly shows that the induction of magnetic field is dominated by large scale flow structures. Especially for the smaller scales of magnetic field, this result implies that the inductive energy transfer is dominated by non-local interactions. It should be remarked that \mathbf{u}_2 , the mode that most intensively excites the magnetic field does not agree with the peak of the kinetic energy spectrum $E_1^{(u)}$. It seems interesting that weak backscatters from magnetic to kinetic energy are seen at $(j, k) = (2, 2), (5, 5)$. Similar backscatter is observed for $t = 16, 18, 20$.

5. Discussion

In the present study, we investigated the effect of coherent isolated vortices on the excitation process of mag-

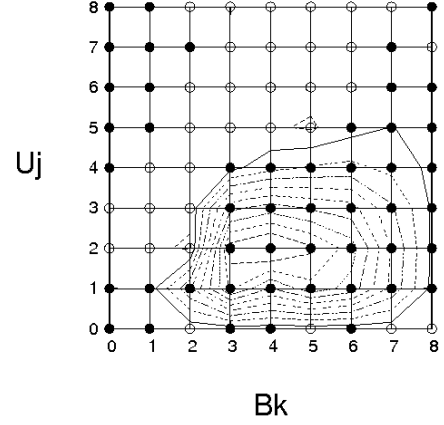


Fig. 6 Wavelet scale spectra of energy transfer from velocity to magnetic field $L_{jk}(= -I_{kj})$. Solid circles: $L_{jk} < 0$, i.e. energy is transferred from \mathbf{u}_j to \mathbf{B}_k ; open circles: $L_{jk} > 0$. Contours are drawn by the same way as Fig.5.

netic field under the existence of uniform background magnetic field. Wavelet analysis of energy redistribution process via the nonlinear and induction/Lorentz force term shows that the motion of fluid is dominated by local interactions while the magnetic field is induced mainly by the large scale fluid motions.

The small scale fluid motions are enhanced by all the terms, i.e. nonlinearity, Lorentz force and Alfvén waves. This implies that MHD dynamics may promote the development of turbulent fluid motion, which is characterized by the highly excited small scale fluid motions.

In the present study we used only the information on the spatial scale of wavelets. Wavelet scale-to-scale analysis of the energy transfers gives consistent results to Fourier ones. Analysis using the spatial location information of wavelets, which is expected to clarify the relation between coherent structures and energy transfers in detail, is now underway.

- [1] D. Biskamp, *Nonlinear Magnetohydrodynamics*, (Cambridge Univ. Press, Cambridge, 1997).
- [2] U. Frisch, *Turbulence*, (Cambridge Univ. Press, Cambridge, 1996).
- [3] M. Lesieur, *Turbulence in Fluids* 4th Ed., (Springer, Dordrecht, 2008).
- [4] C. Canuto et al., *Spectral Methods in Fluid Dynamics*, (Springer, New-York, 1988).
- [5] K. Kishida, K. Araki, K. Suzuki, and S. Kishiba, *Phys. Rev. Lett.*, **83**, 5487 (1999).
- [6] A. Alexakis, P. D. Mininni, and A. Pouquet, *Phys. Rev. E*, **72**, 046301 (2005).
- [7] P. D. Mininni, A. Alexakis, and A. Pouquet, *J. Plasma Phys.*, **73**, 377 (2007).
- [8] K. Araki and H. Miura, "Orthonormal Divergence-free Wavelet Analysis of Nonlinear Energy Transfer in Rolling-Up Vortices", Y. Kaneda (ed.), IUTAM symposium on Computational Physics and New Perspectives in Turbulence, 149 (2008).